Received: 31 October 2021 | Revised: 25 March 2022 | Accepted: 28 April 2022

Life Cycle & Sustainability

Regionalized chemical footprint method to identify aquatic ecotoxicity hotspots of hard disk drive rare-earth magnets

Kali Frost[1] *and Inez Hua*[1,2]

[1]*The Division of Environmental and Ecological Engineering, Purdue University, West Lafayette, Indiana, USA*
[2]*The Lyles School of Civil Engineering, Purdue University, West Lafayette, Indiana, USA*

Abstract

The chemical footprint (ChF), which combines life cycle assessment (LCA) and quantitative risk assessment principles, shows promise for exploring localized toxicity impacts of manufacturing processes, which is not achievable with LCA alone. An updated ChF method was applied to the global annual production of a hard disk drive (HDD) rare-earth element (REE) magnet assembly, assuming a supply chain in East and Southeast Asia. Existing REE magnet assembly LCA inventories were combined with supplier manufacturing locations to create a cradle-to-gate spatial unit process inventory. Emissions from the electricity grid for each manufacturing site were downscaled to hydrobasins of interest using the Global Power Plant Database. The predicted no effect concentration (PNEC) was chosen as the ecotoxicity pollution boundary to determine the threshold for dilution of each chemical of concern (CoC) and to calculate the ChF. Finally, a high-resolution hydrological database provided volumes of the freshwater river reach draining each hydrobasin and was used to calculate the dilution capacity (DC), that is, the volume required to remain at or below the PNEC for each CoC. The total ChF of annual REE magnet assembly production was 6.91E12 m^3, with hotspots in watersheds in China and Thailand where REEs are processed and steel metalworking takes place. Metals were the primary CoCs, with cadmium and chromium(VI) comprising 77% of total ChF. Dilution factors ranged from 5E−09 to 9E + 03 of the DC of the waterbody, reflecting the spatial variability in both emissions and DC. An advanced ChF method was demonstrated for HDD REE magnets. Scoping is a key step required to reduce model complexity. The use of regionalized fate factors and standardized hydrological data sets improves the comparability of ChFs across hydrobasins. Additional work to combine data sets into readily available tools is needed to increase usability and standardization of the ChF method and promote wider adoption. *Integr Environ Assess Manag* 2023;19:272–283. © 2022 The Authors. *Integrated Environmental Assessment and Management* published by Wiley Periodicals LLC on behalf of Society of Environmental Toxicology & Chemistry (SETAC).

KEYWORDS: Aquatic ecotoxicity, chemical footprint, hydrobasin, life cycle assessment, rare earth

INTRODUCTION

Applications and production of rare-earth elements

Rare-earth elements (REEs) are vital to the production of many electronic products including hard disk drives (HDDs), electric vehicles, wind turbines, and light-emitting diodes. The HDD industry is a major consumer of REE permanent magnets and, thus, there has been great interest in quantifying the environmental impacts of HDD REE magnet production (Arshi et al., 2018; Jin et al., 2018; Sprecher et al., 2014). China (58%), the United States (U.S.) (27%), Myanmar (13%), and Australia (7%) are the only countries currently mining notable amounts of REEs (Gambogi, 2021).

Light rare-earth elements (LREEs) such as neodymium and praseodymium are now the dominant REE metals found in HDD magnets. A majority of the world's LREEs are mined from the monazite and/or bastnasite deposits within the Bayan Obo mining region of China. Beneficiation and further processing to REE oxides and metals occur nearby in Baotou, located 150 km south of the Bayan Obo mine. This region in Inner Mongolia currently accounts for 60% of allocated Chinese LREE production (Hu, 2020), and the associated environmental and social impacts from REE extraction and processing in this area have been well publicized (Bontron, 2012). Figure 1 shows the process flow diagram, including REE extraction, production of neodymium, iron, and boron (NdFeB) magnets, and the voice coil magnet assembly (VCMA).

This article contains online-only Supporting Information.

Correspondence Inez Hua, The Division of Environmental and Ecological Engineering, Purdue University, West Lafayette, IN, USA.
Email: hua@purdue.edu

Published 10 May 2022 on wileyonlinelibrary.com/journal/ieam.

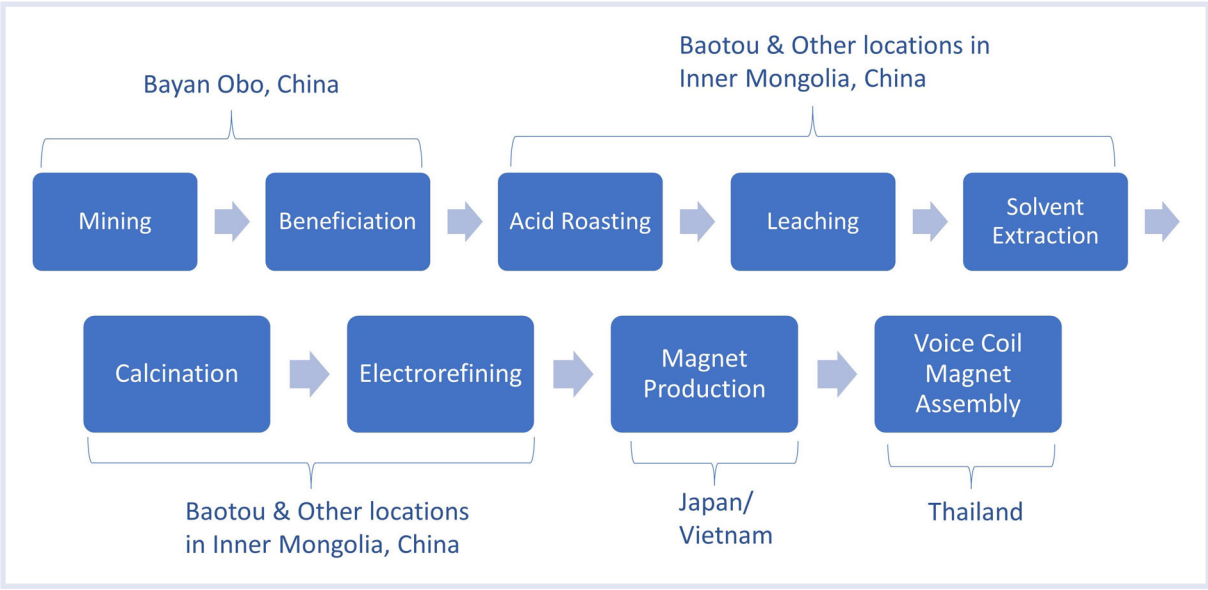

FIGURE 1 Process flow diagram for HDD REE magnets with locations assumed for this study (adapted from Bailey et al., 2020; Frost et al., 2021). HDD, hard disk drive; REE, rare-earth element

Human and ecotoxicity of REE mining and/or processing

Previous life cycle assessment (LCA) work has characterized the human and ecotoxicity impacts from Chinese REE production processes, which is primarily attributed to rare-earth oxide solvent extraction (Bailey et al., 2020). Use of LCA data to quantify the chemical toxicity of products and processes is well established and relies on the toxicity characterization factors from the USEtox database, a United Nations Environmental Program-Society of Environmental Toxicology and Chemistry (UNEP-SETAC) consensus model that includes fate, exposure, and effect parameters for hundreds of substances (Fantke, 2017).

In addition to toxicity impacts modeled through LCA, direct measurements of waterbodies draining the Bayan Obo REE mining and processing sites indicate that toxic levels of metals (e.g., Cr, Cd, and Pb) are accumulating in the environment (Fan et al., 2008; Ma et al., 2016). Many studies also indicate the presence of Radium–226, Thorium–232, and Uranium–238, emitted from both natural and anthropogenic sources (Findeiß & Schäffer, 2017). Process emissions of these radionuclides have been included in REE LCA inventory studies (Lee & Wen, 2016); however, chemotoxicity and radiotoxicity of these substances have only been included in one REE LCA study to date (Bailey et al., 2020), and did not include ecotoxicity impacts.

Life cycle assessment and chemical footprint

While LCA can quantify the amount and types of emissions relative to a functional unit of product, it does little to describe the highly localized relationships between sources and receiving environments (Bare, 2006; Hauschild & Potting, 2005) or account for the impacts of the total volume of emissions (Kara et al., 2018). Thus, a hybridized approach using LCA to determine life cycle emissions and quantitative risk assessment (QRA) to quantify local or regional ecotoxicity impacts may be preferred (de Garcia et al., 2017).

One promising metric for deeper exploration and communication of toxicity impacts is a chemical footprint (ChF). A ChF has been defined as "…a quantitative measure describing the environmental space needed to dilute chemical pollution due to human activities to a level below a specified boundary condition" (Sala & Goralcyk, 2013). ChFs are a part of the footprint family (i.e., carbon, ecological, water footprints), which have been proposed as a method for assessing perturbation of planetary boundaries (Fang & Heijungs, 2014; Posthuma et al., 2014; Vanham et al., 2019) and more robust measurements of a growing, global chemical pollution problem (Landrigan et al., 2018).

The initial application of ChF methods was focused on sector-level, macroscale ecosystem impacts of agricultural and chemical pollutants (Bjorn et al., 2014; Sala & Goralcyk, 2013; Zijp et al., 2014). However, product-level ChFs have been developed more recently for textile and pharmaceutical products, and Li et al. (2021) noted that these studies primarily use a weighted toxicity approach derived from LCA and USETox. Further advancements for regionalizing product ChFs have been proposed (Makarova et al., 2018; Wang, 2019), but a clear path forward has yet to be established.

According to Zijp et al. (2014), the ChF should consider (1) exposure assessment, (2) impact assessment (grounded in traditional risk assessment and LCA principles), (3) boundary conditions (i.e., safe thresholds of pollution defined at local, regional, or global scale [Steffen et al., 2015]), and

(4) the dilution volume needed to maintain the boundary condition, which is a concept introduced by the European Eco-label scheme (1995) and further developed for water footprinting (Hoekstra et al., 2011).

The dilution volume (m^3) of a receiving waterbody is the volume of surface freshwater available to dilute chemical emissions below an ecological or regulatory threshold and relates chemical emissions to the specific dilution capacity (DC) of an aquatic ecosystem (Bjorn et al., 2014; Hoekstra et al., 2011). The emergence of data sets such as HydroATLAS (Linke et al., 2019) makes calculation of an aquatic ecosystem's DC more reliable than previous studies that relied on coarser granularity databases or estimates for volumes of freshwater bodies (Bjorn et al., 2014). HydroATLAS is a database of "hydro-environmental subbasin and river reach characteristics at 15 arc-second resolution," providing consistent calculation of hydrological characteristics and an understanding of upstream and downstream river reach connectivity (Lehner, 2019).

Research gaps and aims

Chemical footprint studies, to date, lack standardized hydrological data as a reference point for calculating DC, a key parameter to assess chemical impact on waterbodies. Further, the global fate and transport factors provided as the default within USETox (Kounina et al., 2014; Rosenbaum et al., 2008) (and therefore LCA software) should be substituted with regionalized fate and exposure factors that have recently become more readily accessible (Verones et al., 2020). Additionally, to the authors' knowledge, downscaling country-level grid mix emissions to allocate a site-specific chemical emissions profile has not been applied within chemical footprinting.

This study applies a regionalized, product-level ChF methodology to explore the aquatic freshwater ecotoxicity of the production of HDD REE magnet assemblies. Because most of the global HDD REE magnet extraction, processing, and assembly occurs within a few known regions, a high-resolution, spatially explicit assessment is possible, and should highlight any toxicity hotspots from virgin REE magnet production, and how it relates to existing aquatic ecosystem carrying capacity.

This study also aims to advance regionalized, product-level ChF methods in several ways:

1. High-resolution emissions data from a Global Power Plant Database (GPPD; Byers et al., 2018) will be used to downscale electricity grid emissions to a watershed (i.e., hydrobasin) level.
2. Use of regional fate and exposure factors for chemicals of concern (CoCs) from USETox and/or LC-IMPACT and estimated impacts for radionuclides on aquatic ecosystems using newly calculated factors.
3. Implement state-of-the-art hydrological data for consistent and accurate calculation of dilution volumes per river reach.

METHODS

This study followed the major analysis steps outlined by Zijp et al. (2014) and the methodology developed by Bjorn et al. (2014) for combining LCA and USETox data to derive a ChF. Figure 2 provides an overview of the major methodological steps and the data sources and transformations performed.

Target and scope

The target product or "functional unit" for this study is a set of REE magnet assemblies (VCMA from a 16TB enterprise HDD, described by Frost et al. [2021]). The REE magnet assembly examined in this study was considered a reasonable proxy for other HDD magnet assemblies currently in production.

There were several scoping steps within the study, namely, (i) geographic scoping (hydrobasin boundary of the receiving body), (ii) CoCs, and (iii) the product system boundary.

System boundary and spatiotemporal scale. This was a cradle-to-gate LCA; however, transportation impacts between manufacturing locations were not considered. Figure 1 shows the production processes included in the system. This study assessed emissions to air, soil, and water, which would be transferred to freshwater ecosystems (rivers and lakes), but did not consider emissions to seawater. Emissions were calculated based on annual production volumes of HDDs (and their mass of associated magnet assemblies). This was determined using the 2019 global annual sales data for HDDs where 260 300 000 HDDs (Coughlin, 2019) contain approximately 27 000 tons of HDD REE magnet assemblies.

Quantification of emissions.

LCA unit process inventory—Step 1. To construct the detailed unit process (UP) data required for a spatially explicit assessment, UP inventory data from Bailey et al. (2020) were used to build the life cycle inventory for the mining, beneficiation, acid roasting, leaching, and solvent extraction processes. Inventory data from Arshi et al. (2018) were used for the conversion of REE oxides into REE metal processing steps, and finally, data from Jin et al. (2020) and Frost et al. (2021) were used to construct processes for neodymium, iron, and boron (NdFeB) magnet production and VCMA manufacturing (i.e., final product assembly where the magnet is epoxied into the steel bracket). In total, 95 unit production processes were used to create the UP inventory (Step 1 of Figure 2). The Ecoinvent v3 database, a widely implemented LCA inventory database, was used to create all inputs and was modeled within Simapro software v8.5.2 (Pre Consultants, 2018). Table S1 presents the complete life cycle inventory and associated data sources.

Emissions inventory—Step 2. The emissions inventory for each UP, which describes emissions to land, water, and air per substance, was exported from Simapro and compiled in

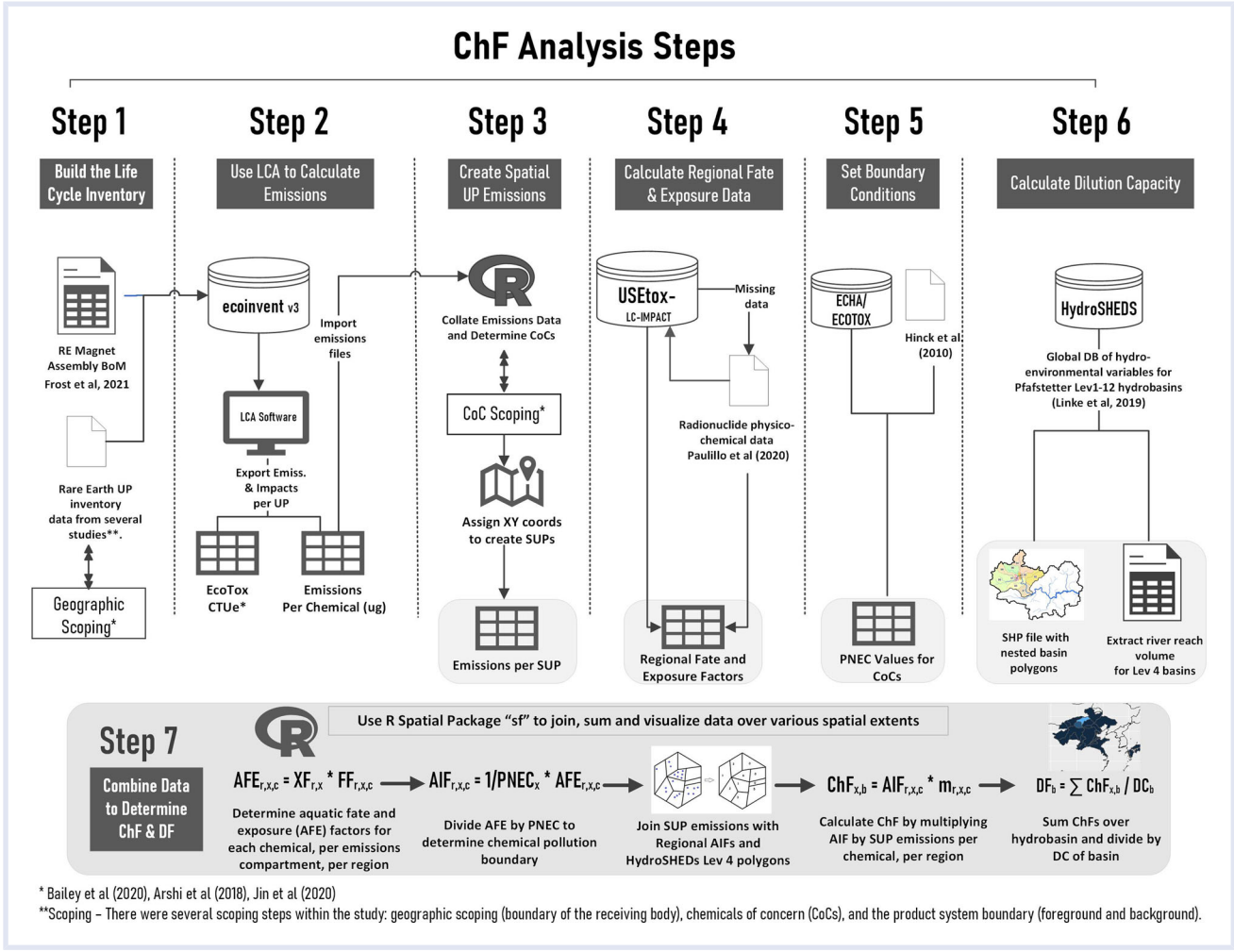

FIGURE 2 Summary of the major methodological steps used in this study and the data sources and transformations performed. This methodology can be applied to any manufactured product, by adjusting Step 1 to include the product-specific Bill of Materials and supply chain (i.e., geographic scoping)

R to summarize emissions per UP (in kg). R is specialized software for statistical computing and graphics (R Core Team, 2017). A screening-level ecotoxicity impact assessment was also used to narrow the emissions inventory to a smaller list of CoCs for further ChF analysis. The cut-off for inclusion in the CoC list was a 0.01% contribution to total aquatic ecotoxicity, expressed in comparative toxic units for aquatic ecotoxicy (CTU), which aligns with the recommendation from USETox to include any chemical representing greater than 1/1000th contribution to toxicity for in-depth analysis (Fantke, 2017). Nineteen chemicals (17 metals and two organics) were selected as CoCs and for an additional three substances, Thorium—232, Uranium—238, and Radium—226, there were no ecotoxicity data in USEtox, but these were included as CoCs because of concerns with radioactive emissions from REE mining and processing (Bailey et al., 2020; Findeiß & Schäffer, 2017; Lee & Wen, 2016).

Assigning spatial unit processes—Step 3.

Manufacturing materials. Manufacturing locations along the REE magnet life cycle were taken from the literature (Bailey et al., 2020; Frost et al., 2021). Manufacturing occurs in more than one location for some of the UPs, and emissions were allocated based on approximate production volumes for each site where locations were known. Each UP was assigned latitude–longitude coordinates and became part of the "Spatial Product System" (Marzullo et al., 2018), referred to herein as a spatial UP, or SUP. The manufacturing locations described in this study can be considered a theoretical supply chain for REE magnet assemblies based on a combination of known existing supplier locations, but it is not inclusive of all the possible manufacturing locations for this product.

Steel manufacturing emissions. One of the major contributors to ecotoxicity impacts is from the engineered steel bracket ("iron yoke"), which houses the REE magnet (Frost et al., 2021). This is the largest component in the assembly, with a mass of 72.6 g (combined mass of upper and lower yokes), compared to 31.2 g for the REE magnets. Thus, both the engineered steel and stainless steel that comprise the yoke were considered to be a high-impact material, and

further disaggregation of the likely steel supply chain was needed to understand the spatial variation of impacts related to its production. The REE magnet is adhered to the yoke in Thailand, but the steel material for the yoke was likely imported, given the low amount of steel production in Thailand, an assumption further justified by the specialty nature of the steel alloy used in these assemblies. The Global Steel Trade Monitor (ITA, 2019) provides import–export data for many of the countries within the global steel exchange markets. The top two trade partners with Thailand are Japan and China. For Japan, the emissions were spatially allocated at the country level, which aligned with the scale of the hydrobasin, and for China, steel production impacts were allocated to the major steel exporting provinces (Worldsteel, 2020). The steel spatial allocation process is fully documented in the Supporting Information.

Electricity.

Chinese electricity emissions. Electricity from the grid is used to supply many of the manufacturing processes in the REE magnet supply chain, so impacts from electricity were allocated to the specific location where power was generated. The GPPD's facility-level, annual generation values (Byers et al., 2018) were used to construct the supply mixes for each of the six electricity grids within the Chinese mainland, following the grid boundaries described in Frost and Hua (2019). This approach is preferred over provincial or regional grid mix estimates provided by the LCA databases because it incorporates a large and representative amount of up-to-date facility-level production data. However, the GPPD data set only supplies generalized fuel types (e.g., hydroelectric, solar, wind, natural gas), so subfuel mixes within a fuel type (e.g., hydroelectric pumped storage vs. hydroelectric run-of-river) were taken from Ecoinvent v3 grid mix profiles (Treyer & Bauer, 2016). A custom UP for each general technology and/or fuel type was then constructed as a weighted average of emissions based on the contribution of each of these subfuel types. Example calculations of the subfuel mix are available in the Supporting Information.

$$FME_{x,f,g} = w_{s,g} \times m_{x,s,g}, \quad (1)$$

where FME is the fuel mix emissions, m is the mass of emissions per CoC (x), per subfuel type (s), and w is the proportion of electricity produced by the subfuel type within a particular electricity grid (g).

Other countries. Due to less geographic variability in grid mixes within Japan and Vietnam and the geographic scope of the receiving watersheds (Figure 3), national-level grid mixes were considered representative for these countries. The electricity grid in Thailand was excluded from this analysis because of the lack of data on electricity consumption in foreground processes for the VCMA manufacturing step. Grid mixes for Japan and Vietnam were derived from International Energy Agency 2019 tables (IEA, 2020) and provide up-to-date data for production capacity by fuel type, per country. Subfuel type mixes for Japan and Vietnam from Ecoinvent v3 were implemented.

Downscaling grid emissions to each power plant facility. Emissions per fuel type (e.g., coal, natural gas, hydroelectric) and per country (or per province, in China) were exported from LCA software, and each fuel mix profile was constructed in R using Equation (1). The electricity usage for each manufacturing step was allocated to each REE manufacturing SUP to understand how much electricity was used in each location. Each SUP was then associated with an electricity grid and spatially joined to the GPPD, where annual generation from individual power plants could be used to downscale the emissions for each fuel mix to the

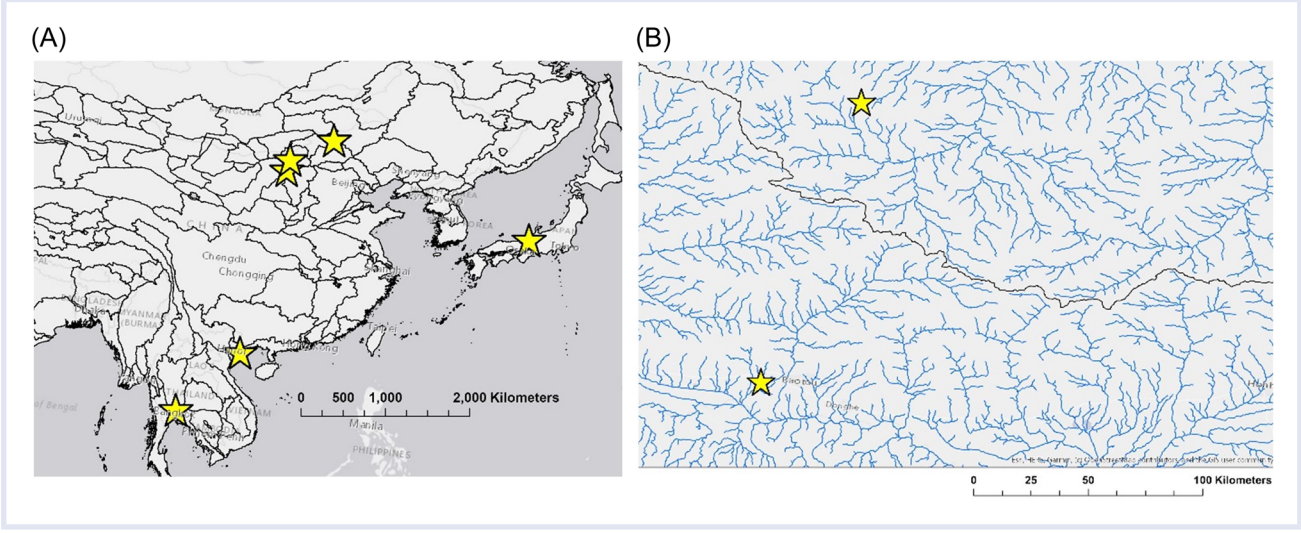

FIGURE 3 (A) (left) shows a map of the Level 4 basins for East Asia available from HydroBASINs with Rare Earth manufacturing locations represented as yellow stars. (B) (right) shows the 15 arc-second resolution river reaches within the Level 4 basin near Bayan Obo, China (top yellow star), and Baotou, China (bottom yellow star)

exact facility locations (and basins) associated with each fuel (Equation 2).

$$PPE_{x,f,g} = FME_{x,f,g} \times w_{i,f,g}, \quad (2)$$

where PPE is the power plant emissions, FME is derived from Equation (1), and w_i is the proportion of total electricity produced by individual power plant (i) of fuel type (f) within grid (g), and x is the CoC.

Summarizing emissions per CoC—Steps 3 and 7. The emissions data for all SUPs, per chemical, can then be summarized over any spatial scale of interest (i.e., Levels 1–12 basins). For the Level 4 basins used in this study, it was assumed that emissions were limited to the basin where the source was located. This may not always be the case for certain source types (e.g., air emissions from power plants) due to wind speed and/or direction and complex atmospheric transport and transformation mechanisms associated with air emissions from tall stacks. However, the geographic scope of the basins used in this analysis (~1E + 04 km^2) encompasses near field dispersion of emissions (<50 km radius from the source) (Perry et al., 2005).

Quantifying fate and exposure of CoCs—Step 4. Regional fate and exposure factors are provided in the LC-IMPACT data set (Verones et al., 2020), which are an extension of USETox v2.12 factors and have been used to determine regionalized exposure data for each CoC. Impact factors for radiological chemicals are not currently integrated into the USETox database, so fate and transport factors were constructed in USETox using physicochemical data from Paulillo et al. (2020), with the assumption that the technically enhanced naturally occurring radioactive materials (TENORMs) assessed in this study behave similarly to metals with respect to solubility and mobility (MDEQ, 2015).

There were three geographic regions of interest in this study with respect to fate and exposure factors: Eastern China, Japan and the Korean peninsula, and Southeast Asia (Vietnam, Malaysia, and Thailand). Regionalized impacts supplied by the LC-IMPACT data set were sometimes 5–10-fold larger than the default, global average factors provided by USETox v2.12, underscoring the need for more spatial granularity in impact assessment. For example, the fate factor for transport of cadmium (Cd^{2+}) from rural air to freshwater is 1.72E + 02 and 3.40E + 01 (d^{-1}) for China and the global average, respectively. Fate and eco-exposure factors per chemical can be summarized using Equation (3), adapted from Rosenbaum et al. (2008).

$$AFE_{r,x,c} = XF_{r,x} \times FF_{r,x,c}, \quad (3)$$

where AFE is the aquatic fate and exposure in kg/day, r is the region of interest, x is the CoC, and c is the environmental compartment (land, air, water) transferring chemicals to freshwater (e.g., continental urban air to freshwater, continental rural air to freshwater).

XF is the regional eco-exposure factor derived in LC-IMPACT (i.e., regionalized USETox), which represents the fraction of chemical dissolved in freshwater (dimensionless) that could impact aquatic freshwater species.

FF is the regional fate factor is the rate of transfer in (d^{-1}) for the transfer of emissions from air, water, and soil to freshwater.

Chemical pollution boundary—Step 5. The chemical pollution boundary or "ecotoxicity effect factors" embedded in USETox are derived using the HC50 (i.e., the concentration at which 50% of the species are exposed above their EC50) and are widely implemented in LCA modeling. However, given the hybridized approach intrinsic to chemical footprinting, there is an opportunity to consider regulatory, risk assessment-based boundaries, such as the no observed effect concentration (NOEC) or the predicted no effect concentration (PNEC). The use of more "average" toxicity factors such as the HC50 versus more sensitive, conservative factors such as the NOEC or PNEC is heavily debated among practitioners of LCA and QRA (Saouter et al., 2017), with five alternative recommendations from these authors for use in the EU's Product Environmental Footprint.

The boundary chosen for this study was the PNEC, which is a "policy" or regulatory boundary (Zijp et al., 2014), and is available from the European Chemicals Agency's (ECHA) database of Registration, Evaluation, Authorization and Restriction of Chemicals registration dossiers (ECHA, 2021). A $PNEC_{freshwater}$ was chosen as the policy boundary because of (a) ready access to freshwater hazard information for a large, standardized, database of chemicals, and (b) calculation of PNECs follows a precautionary principle (Hauschild & Potting, 2005) by selecting the most sensitive species among the available ecotoxicity effect data and applying assessment factors to account for uncertainty (Saouter et al., 2017). However, there are drawbacks to using the PNEC: It does not take into account existing chemical pressures in the receiving waterbody or the specific existing species assemblages and their exposure to a mixture of chemicals (although conservative assessment factors partially account for this uncertainty).

For most of the metals being considered in this study, PNECs are readily available from ECHA or US EPA's ECOTOX database (EPA, 2021). For radionuclides, PNEC data were obtained from Hinck et al. (2010) and are represented by μGy/h. A gray (Gy) is a unit of ionizing radiation defined as the absorption of 1 J of radiation energy per kilogram of matter. For the radionuclides, Radium–226, Thorium–232, and Uranium–238, each chemical is subject to both chemotoxicity and radiotoxicity PNECs. The PNEC is used, along with the AFE (Equation 3), to derive an aquatic impact factor (AIF) per region, per chemical, and per compartment.

$$AIF_{r,x,c} = 1/PNEC_x \times AFE_{r,x,c}, \quad (4)$$

where AIF is the aquatic impact factor, r is the USETox region, x is the CoC, and c is the emissions compartment. AFE

 DOI: 10.1002/ieam.4631

is the aquatic fate and exposure calculated in Equation (3), and $PNEC_x$ is the PNEC for freshwater in μg/L or μGy/h for radionuclides.

Using the results of Equation (4), one can calculate the ChF per chemical using the annualized mass of emissions per region, per chemical, and per compartment.

$$ChF_{r,x,c} = AIF_{r,x,c} \times m_{r,x,c}, \quad (5)$$

where ChF is the chemical footprint in m^3, AIF is the aquatic impact factor from Equation (4), x is the CoC, c is the media compartment (air, water, land), m is the mass of emissions, and r is the regional factor from Verones et al. (2020).

Dilution volume—Step 6.

Hydrobasins of interest. To determine the ChF and DC of emissions, each SUP must be associated with a receiving body of water. The HydroBASINs data set is comprised of hydro-environmental variables such as discharge, land cover, and temperature (Linke et al., 2019). Hydrological data, such as natural discharge, are available via integration of two companion data sets: BasinATLAS and RiverATLAS. BasinATLAS provides the "hierarchically nested subbasins at multiple scales," and RiverATLAS links these to the individual river reaches that drain each basin (Lehner, 2019). Both data sets are available at a highly granular 15 arc-second (~500 m) resolution. Subbasins are delineated using the Pfafstetter system at Levels 1–12, which are derived from high-resolution topography data (Linke et al., 2019), where Level 1 represents continental-scale watersheds and Level 12 is ~1E + 02 km^2. Application basins (~1E + 04 km^2) were selected as the geographic scope of interest for this study because they represented a suitable compromise between spatial granularity and a practical geographic scope relative to the emissions sources. Figure 3 shows the Level 4 hydrobasins used in this study, as well as the high-resolution river reach data used to calculate the DC of the receiving body.

Mapping SUP emissions to hydrobasins. The latitude–longitude coordinates assigned to each SUP were used to spatially join emissions with the corresponding Level 4 HydroBASIN data set, using the "sf" library in R (Pebesma, 2018). Level 4 was chosen as the scale for this study; however, the results could be aggregated or disaggregated to suit various hydrobasin levels.

HydroBASINs provide data on the natural discharge in m^3/s of each river reach upstream of a subbasin pour point (i.e., junction of a stream network) (Lehner, 2019). River reach discharge is calculated in HydroBASINs using the globally integrated water balance model WaterGAP, which is downscaled to the 15 arc-second (~500 m) resolution of the HydroSHEDS river network (Lehner & Grill, 2013).

Relating ChF to local DC—Step 7. A ChF for each CoC can be calculated by multiplying the regional AIF_r by the emissions of the CoC over a given boundary for a length of time. The boundary for this study is a Level 4 basin, and the emissions occur over one year of production. To relate the ChF to the receiving body's DC, we must sum the footprints of all chemicals within the basin and divide this by the total annual DC (annual river volume) of the river reach that drains the basin. This results in a dilution factor (DF), which is the amount of the annual volume needed to dilute the CoC to the PNEC. A DF > 1 indicates that the volume required to dilute the CoCs exceeds the capacity of the waterbody, and DF < 1 means that there is enough freshwater available to dilute the CoC to a safe threshold for aquatic life. This is similar to the process to calculate the gray water footprint, or "critical load approach"; however, this DF calculation does not take into account the existing natural background concentrations of each chemical (Hoekstra et al., 2011).

$$DF_b = \frac{\sum_x ChF_{b,x}}{DC_b}, \quad (6)$$

where DF is the dilution factor; ChF is from Equation (5), summed over the basin of interest (b), for each CoC (x).

RESULTS AND DISCUSSION

Chemical footprint

The cumulative ChF of all CoC emissions to air, soil, and water across the cradle-to-gate REE magnet manufacturing life cycle was 6.91E + 12 m^3 of freshwater per year. This impact is associated with an annual production of ~27 000 tons of HDD RE magnet assemblies. It can be difficult to compare ChFs across studies due to differences in the magnitude of emissions, relative toxicity of the CoCs, and geography; however, ChFs reported by Bjorn et al. (2014) and Zijp et al. (2014) for pesticide ecotoxicity in European watersheds indicated a range from 3.0E + 9 to 1.1E + 12 m^3.

To understand impacts relative to manufacturing locations and their associated receiving bodies, ChF emissions were also summarized for each Level 4 basin impacted by primary magnet assembly production (Scope 1) *and* electricity associated with production (Scope 2).

Primary magnet manufacturing emissions occurred in nine Level 4 basins, with impacts predominating in the basins associated with REE processing (Baotou & Inner Mongolia-at large) and VCMA manufacturing (Pathum Thani, Thailand) (Figure 4A). The impact of VCMAs is due to steel metalworking processes required to shape the steel yoke that are assumed to occur in Thailand. Figure 4B shows the ChFs summarized by each major production unit, showing the impacts of the steel metalworking (VCMA) and the various REE separation processes including acid roasting and solvent extraction (depicted in "Pr Oxide," "Nd Oxide," and "REE sulfate from acid roasting 50 perc" in Figure 4A).

Dilution factor

When comparing the ChF in each hydrobasin to the DC of its associated freshwater receiving body, the largest impacts were in Thailand, Bayan Obo (Inner Mongolia), and Jiangsu and Shandong provinces in China. The DF is used to reflect

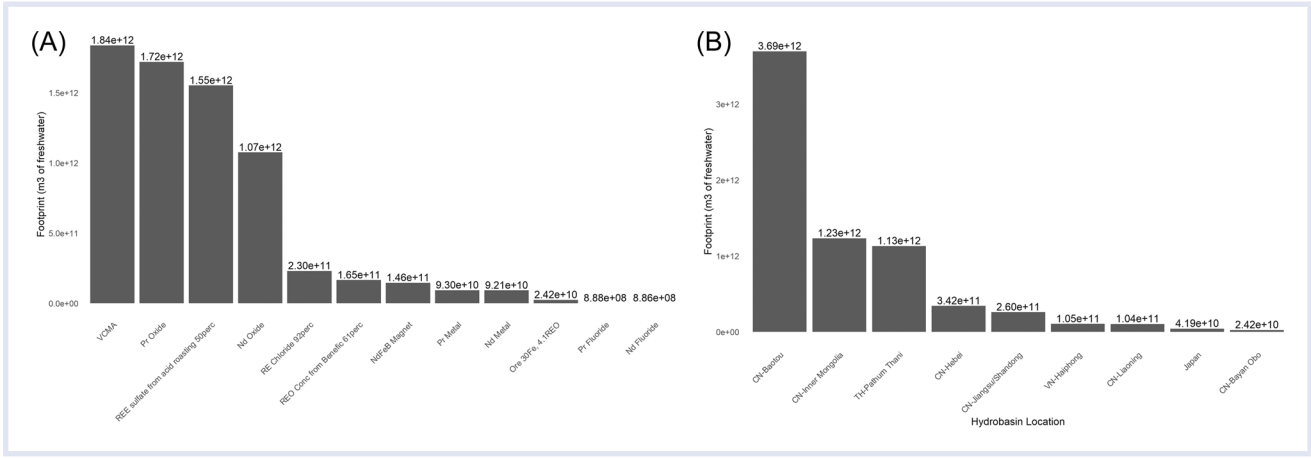

FIGURE 4 Chemical footprint in m^3 from Scope 1 magnet manufacturing emissions by basin of interest (A) and by each major production unit (B). The labels for each basin represent a general description of the geographic area (city, province, or country) where the manufacturing occurs, based on the granularity of location data available

the volume of the receiving body and its ability to assimilate chemical emissions. Figure 5A shows the DF required to dilute the annual emissions from magnet processing (Scope 1) to the PNEC for CoCs within the river reach directly draining each watershed.

Dilution factors for these watersheds are very high in some cases, with an average DF of 2480 times the available annual dilution volume. This is likely due to several factors:

1. The CoCs in this study are almost exclusively metals, which are highly toxic to aquatic organisms (PNECs ~ 1E−9 g/L), corresponding to a large ChF. In line with LCA and/or QRA principles, chemical toxicity is considered in an additive manner, which is meant to consider the co-exposure of chemicals with similar modes of action (Saouter et al., 2017), but compounds the conservative uncertainty (i.e., safety) factors that are already applied in PNEC calculations. Several authors have noted the large uncertainty introduced by toxicity parameters and the sensitivity of ChF methods to this parameter (Bjorn et al., 2014; Fantke, 2017; Saouter et al., 2017).
2. Several of the watersheds under consideration are located in semiarid to arid climates, which may have very little average annual natural discharge (e.g., 0.4 m^3/s). As such, these areas likely require different management of process waste in the facility (e.g., significant reduction in chemical concentrations before emission to waterbodies), and may have contributions to flow from anthropogenic discharge, but this is not taken into consideration by current assumptions.

When electricity-related impacts (Scope 2) were also considered, the number of impacted watersheds expanded to 32, due to the large number of watersheds associated with electricity production. Electricity emissions and impacts are generally lower than those associated with materials and processing, and more dispersed within China due to the allocation of electricity impacts across

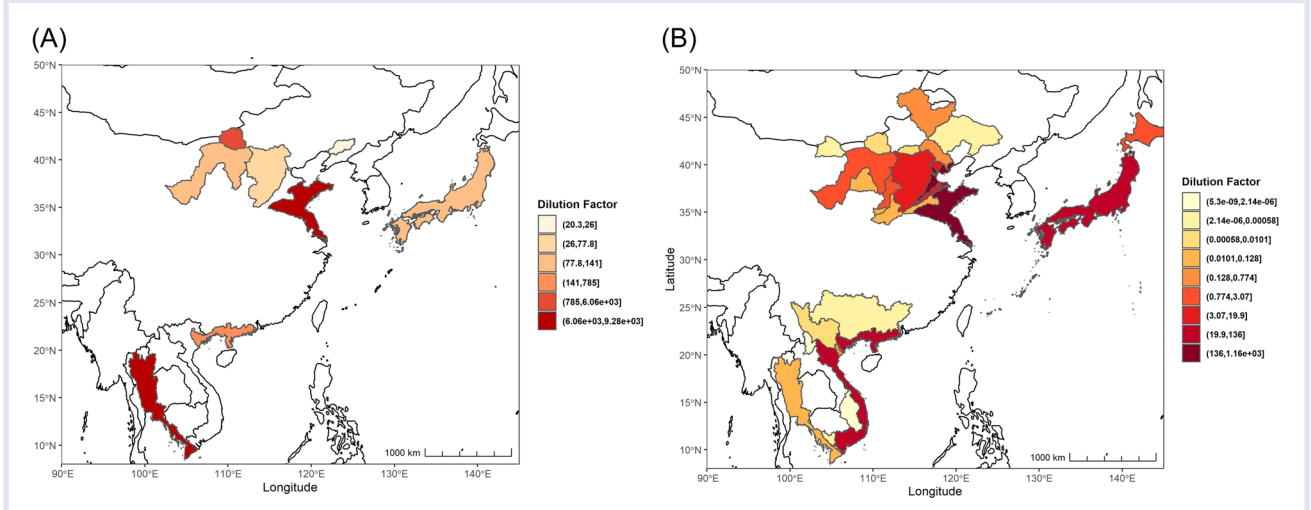

FIGURE 5 Dilution factors of the river reach required to dilute the sum of each of the chemicals of concern to its PNEC for locations associated with (A) REE magnet processing (Scope 1) and (B) process electricity use (Scope 2). REE, rare-earth element

 DOI: 10.1002/ieam.4631

TABLE 1 Radiotoxicity and chemotoxicity footprints of three radionuclides associated with rare-earth element mining and processing

Chemical substance	Chemotoxicity footprint (m^3)	Radiotoxicity footprint (m^3)
Radium–226	4.04E−14	1.20E−12
Thorium–232	5.99E−22	1.06E−13
Uranium–238	7.52E−19	6.55E−11

several hydrobasins located within the grid. Figure 5B shows the DF required to dilute the annual emissions from electricity use associated with REE magnet manufacturing (Scope 2) to the PNEC for CoCs within the river reach directly draining each watershed. Full results are presented in Table S8.

Chemical footprint by TENORMs

The total ChF by TENORMs was a minor contributor to the ChF (Table 1), when compared to toxicity from metals. This is due to calculations for fate and transport, driven by the extremely low solubility and mobility of these chemicals.

However, significant concentrations of these chemicals are present in nearby freshwater bodies due to migration from waste piles and mining and/or processing tailings ponds, with concentrations of thorium measured at up to 5 mg/L in leaching ponds and 0.1–1 μg/L in remote freshwater sites (Findeiß & Schäffer, 2017) near Baotou REE processing facilities. Current LCA emissions and transport modeling data may be an inadequate tool to describe the risk from these TENORMS, especially due to lack of integration of effluent pH and soil-specific mobility concerns (Findeiß & Schäffer, 2017), which are not addressed by generalized TENORM physicochemical data.

Contribution Per CoC

Ecotoxicity impacts were dominated by just a handful of metals associated with REE manufacturing and metalworking. Chromium (VI) was the largest impact driver, accounting for 56.1% of the ChF, followed by cadmium (20.6%) and nickel (11.3%). Impacts per CoC are somewhat variable over hydrobasins (Figure 6), with a different emissions composition from REE processing (i.e., Baotou, China) and steel metalworking (i.e., Pathum Thani, Thailand).

Predicted versus sampled concentrations of CoCs

Predicted emissions from the magnet manufacturing processes and their associated concentration in receiving bodies can be compared to sampling data available for the Yellow River, at locations just downstream of the Baotou processing facilities. For example, concentrations of Cd at these sites ranged from 0.1 to 4.3 μg/L in water and from 0.16 to 0.53 mg/kg in sediment, respectively (Fan et al., 2008; Ma et al., 2016), compared to modeled concentrations of 6.75 μg/L in water (Table 2).

Although these monitored concentrations are within the correct order of magnitude, using LCA data to predict in-stream concentrations may be problematic because: (1) although the goal was to elucidate the impact of HDD magnets, these magnets only comprise a portion of the LREE metals mining and processing in this area, and annual mining and processing quotas may be a better indicator of total burden for the Baotou site, in particular, (2) LCA and USETox modeling relies on steady-state assumptions of emissions, which does not account for the cumulative contamination from persistent, metals from years of mining, processing, and slag storage in this area and the ongoing exchange between sediment-bound metals and overlying waters, and (3) the natural background levels of metals in water at this location that are not accounted for in the USETox modeling. These issues are true for all LCA-derived

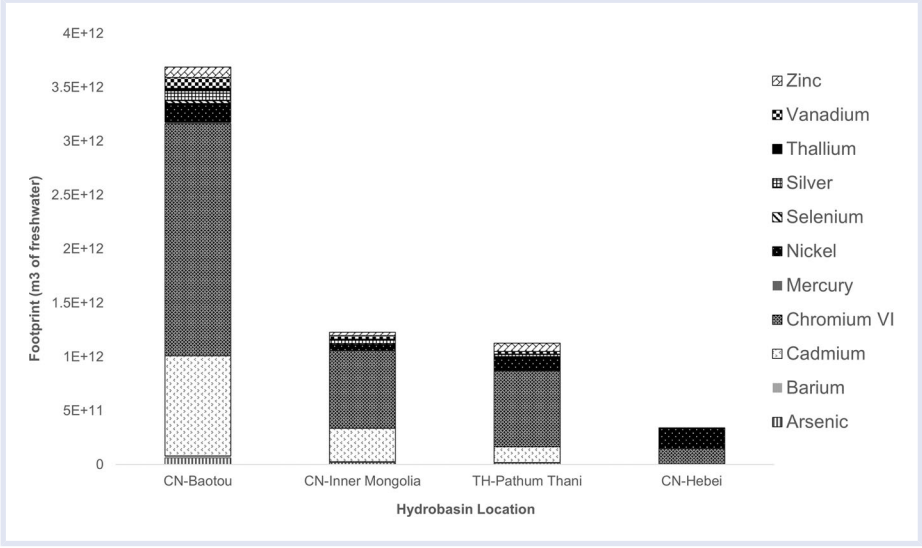

FIGURE 6 Chemical footprint for each hydrobasin, showing contribution by chemicals of concern (CoCs). This figure excludes CoCs, which contribute less than 2% of the total footprint, to improve clarity

TABLE 2 Modeled concentrations versus selected monitoring data from the Yellow River near Baotou, China REE processing facilities

Chemical of concern	Modeled concentration (μg/L)	Sampled concentrations		
		Water (μg/L)[a]	Sediment[b] (mg/kg)	Sediment background[b] (mg/kg)
Chromium (VI)	3.85	N/A	90	41.4–70.2
Cadmium	6.75	0.1–4.3	0.16–0.53	0.1
Nickel	47.2	N/A	15	19.5–36.6
Zinc	74.2	2.8–227	50	58.8–68.5

Abbreviation: REE, rare-earth element.
[a]Fan et al. (2008).
[b]Ma et al. (2016).

emissions and underscore the difficulty of using LCA-derived ChF data to predict concentrations at a particular time and space, rather than as a tool to predict *potential* total ecotoxicity impact.

CONCLUSIONS

This study quantified the freshwater ecotoxicity footprint of producing HDD REE magnet assemblies on the waterbodies associated with manufacturing facilities within a theoretical supply chain. Twenty-three CoCs were identified using the UP emissions data available from the LCA literature. Metals were the dominant drivers of ecotoxicity impact, and the three radionuclides of concern were relatively minor by comparison, but may be inadequately represented by nonspecific fate and transport factors and an underestimate of emissions. The results demonstrate the applicability of a novel chemical footprinting methodology to a specific product. To reduce the analytical burden of conducting ChFs generally, we recommend the development of a geographic information system-based tool that can link regional USETox fate and exposure factors, their associated PNECs, and global HydroBASINs data including discharge volumes for river reaches at various spatial scales. This compiled information, when coupled with location-specific emissions (from LCA or directly from facilities), should provide the inputs to calculate a robust, location-specific, ChF for a variety of products.

The ChF method provides insights beyond typical LCA by placing emissions and impact within the context of the local receiving body (i.e., source–receptor pathway in QRA). This is important for many products that have known aquatic toxicity concerns, and ChFs have been conducted for pesticides, textiles, detergents, and pharmaceuticals to date. In the case of HDD magnet assemblies, metal toxicity from steel manufacturing and REE processing was shown to be impactful, but the main location for REE processing (in Baotou, China) was less impactful than its footprint might suggest due to the high discharge volume of the Yellow River near Baotou processing facilities. By factoring in the DC of a given receiving body, stakeholders can target the most vulnerable ecosystems with respect to these products, although existing vulnerability due to historic pollution should be considered as well.

Ongoing work and future development of local and regionalized planetary boundaries for environmental impact categories, including chemical toxicity (Bjorn et al., 2020), should help organizations to develop science-based targets for toxicity reduction in their products or processes. A standardized, spatially explicit chemical footprinting methodology may play a vital role in quantifying an organization's impact and their contribution to or exceedance of local or regional planetary boundaries. To this end, this work aims to further develop and standardize the methodology, but there are still areas for improvement with regard to modeling variability in specific source–receptor interactions, accounting for existing chemical pressures in a waterbody, and linking with robust, aquatic biodiversity data.

ACKNOWLEDGMENT

The authors acknowledge the support of the Purdue Doctoral Fellowship for their generous funding of this work.

CONFLICT OF INTEREST

The authors declare no conflicts of interest.

DATA AVAILABILITY STATEMENT

The supporting data for this manuscript are available in the Supporting Information.

SUPPORTING INFORMATION

The xlsx file contains data tables supporting the calculations and figures provided in the manuscript. The word document contains detailed methods with example calculations.

ORCID

Kali Frost http://orcid.org/0000-0003-2493-5065
Inez Hua http://orcid.org/0000-0003-4977-5758

REFERENCES

Arshi, P. S., Vahidi, E., & Zhao, F. (2018). Behind the scenes of clean energy: The environmental footprint of rare earth products. *ACS Sustainable Chemistry & Engineering*, *6*(3), 3311–3320. https://doi.org/10.1021/acssuschemeng.7b03484

Bailey, G., Joyce, P. J., Schrijvers, D., Schulze, R., Sylvestre, A. M., Sprecher, B., & Van Acker, K. (2020). Review and new life cycle assessment for rare earth production from bastnäsite, ion adsorption clays and lateritic

monazite. *Resources, Conservation And Recycling*, *155*, 104675. https://doi.org/10.1016/j.resconrec.2019.104675

Bare, J. C. (2006). Risk assessment and life-cycle impact assessment (LCIA) for human health cancerous and noncancerous emissions: integrated and complementary with consistency within the USEPA. *Human and Ecological Risk Assessment*, *12*(3), 493–509.

Bjørn, A., Diamond, M., Birkved, M., & Hauschild, M. Z. (2014). Chemical footprint method for improved communication of freshwater ecotoxicity impacts in the context of ecological limits. *Environmental Science & Technology*, *48*(22), 13253–13262. https://doi.org/10.1021/es503797d

Bjørn, A., Sim, S., King, H., Patouillard, L., Margni, M., Hauschild, M. Z., & Ryberg, M. (2020). Life cycle assessment applying planetary and regional boundaries to the process level: A model case study. *The International Journal of Life Cycle Assessment*, *25*(11), 2241–2254. https://doi.org/10.1007/s11367-020-01823-8

Bontron, C. (2012, August 7). Rare-earth mining in China comes at a heavy cost for local villages. *The Guardian*. https://www.theguardian.com/environment/2012/aug/07/china-rare-earth-village-pollution

Byers, L., Friedrich, J., Hennig, R., Kressig, A., Li, X., Valeri, L. M., & McCormick, C. (2018). *A global database of power plants*. Washington, DC: World Resources Institute. Available online at www.wri.org/publication/global-database-power-plants

Coughlin, T. (2019, February). 2018 Hard disk drive results. *Forbes*. https://www.forbes.com/sites/tomcoughlin/2019/02/04/2018-hard-disk-drive-results/#3c1f8df745a7

ECHA. (2021). ECHA registered substances. https://echa.europa.eu/fr/information-on-chemicals/registered-substances

EPA. (2021). ECOTOX Knowledgebase. https://cfpub.epa.gov/ecotox/search.cfm

Fan, Q., He, J., Xue, H., Lü, C., Sun, Y., Shen, L., & Bai, S. (2008). Heavy metal pollution in the Baotou section of the Yellow River, China. *Chemical Speciation & Bioavailability*, *20*(2), 65–76. https://doi.org/10.3184/095422908X322824

Fang, K., & Heijungs, R. (2014). There is still room for a footprint family without a life cycle approach—comment on "Towards an Integrated Family of Footprint Indicators". *Journal of Industrial Ecology*, *18*(1), 71–72. https://doi.org/10.1111/jiec.12067

Fantke, P. (2017). USEtox® 2.0 Documentation (Version 1). http://usetox.org

Findeiß, M., & Schäffer, A. (2017). Fate and environmental impact of thorium residues during rare earth processing. *Journal of Sustainable Metallurgy*, *3*(1), 179–189. https://doi.org/10.1007/s40831-016-0083-3

Frost, K., & Hua, I. (2019). Quantifying spatiotemporal impacts of the interaction of water scarcity and water use by the global semiconductor manufacturing industry. *Water Resources and Industry*, *22*(3), 100115. https://doi.org/10.1016/j.wri.2019.100115

Frost, K., Sousa, I., Larson, J., Jin, H., & Hua, I. (2021). Environmental impacts of a circular recovery process for hard disk drive rare earth magnets. *Resources, Conservation And Recycling*, *173*, 105694. https://doi.org/10.1016/j.resconrec.2021.105694

Gambogi, J. (2021, January). Rare Earths. U.S. Geological Survey, Mineral Commodity Summaries. https://pubs.usgs.gov/periodicals/mcs2021/mcs2021-rare-earths.pdf

de García, S. O., García-Encina, P. A., & Irusta-Mata, R. (2017). The potential ecotoxicological impact of pharmaceutical and personal care products on humans and freshwater, based on USEtox™ characterization factors. A Spanish case study of toxicity impact scores. *Science of the Total Environment*, *609*, 429–445. https://doi.org/10.1016/j.scitotenv.2017.07.148

Hauschild, M., & Potting, J. (2005). Spatial differentiation in life cycle impact assessment—the EDIP2003 methodology. *Environmental News*, *80*, 1–195.

Hinck, J. E., Linder, G., Finger, S., Little, E., Tillitt, D., & Kuhne, W. (2010). Biological pathways of exposure and ecotoxicity values for uranium and associated radionuclides. In *Hydrological, geological and biological site characterization of Breccia Pipe uranium deposits in Northern Arizona*. U.S. Geological Survey, Scientific Investigations Report, 5025.

Hoekstra, A. Y., Chapagain, A. K., Aldaya, M. M., & Mekonnen, M. M. (2011). The water footprint assessment manual: Setting the global standard. Washington D.C.: Earthscan. https://waterfootprint.org/media/downloads/TheWaterFootprintAssessmentManual_2.pdf

Hu, T. (2020, July 16). China's rare earth mining quota for 2020 up 6% YOY. *S&P Global Market Intelligence*. https://www.spglobal.com/marketintelligence/en/news-insights/latest-news-headlines/china-s-rare-earth-mining-quota-for-2020-up-6-yoy-59452763

IEA. (2020). Electricity generation by source [Table]. Retrieved tables for Japan, Vietnam and Thailand. https://www.iea.org/fuels-and-technologies/electricity

ITA. (2019, March). Steel imports report: Thailand. Global Steel Trade Monitor. https://legacy.trade.gov/steel/archives/index.asp

Jin, H., Afiuny, P., Dove, S., Furlan, G., Zakotnik, M., Yih, Y., & Sutherland, J. W. (2018). Life cycle assessment of neodymium-iron-boron magnet-to-magnet recycling for electric vehicle motors. *Environmental Science & Technology*, *52*(6), 3796–3802. https://doi.org/10.1021/acs.est.7b05442

Jin, H., Frost, K., Sousa, I., Ghaderi, H., Bevan, A., Zakotnik, M., & Handwerker, C. (2020). Life cycle assessment of emerging technologies on value recovery from hard disk drives. *Resources, Conservation & Recycling*, *157*, 104781. https://doi.org/10.1016/j.resconrec.2020.104781

Kara, S., Hauschild, M. Z., & Herrmann, C. (2018). Target-driven life cycle engineering: Staying within the planetary boundaries. *Procedia CIRP*, *69*, 3–10. https://doi.org/10.1016/j.procir.2017.11.142

Kounina, A., Margni, M., Shaked, S., Bulle, C., & Jolliet, O. (2014). Spatial analysis of toxic emissions in LCA: A sub-continental nested USEtox model with freshwater archetypes. *Environment International*, *69*, 67–89. https://doi.org/10.1016/j.envint.2014.04.004

Landrigan, P. J., Fuller, R., Acosta, N. J., Adeyi, O., Arnold, R., Baldé, A. B., & Chiles, T. (2018). The Lancet Commission on pollution and health. *The Lancet*, *391*(10119), 462–512. https://doi.org/10.1016/S0140-6736(17)32345-0

Lee, J. C., & Wen, Z. (2016). Rare earths from mines to metals: Comparing environmental impacts from China's main production pathways. *Journal of Industrial Ecology*, *21*(5), 1277–1290. https://doi.org/10.1111/jiec.12491

Lehner, B. (2019, December). *HydroATLAS: A global compendium of hydro-environmental sub-basin and river reach characteristics at 15 arc-second resolution*. Technical Documentation Version 1.0. https://www.hydrosheds.org/page/hydroatlas

Lehner, B., & Grill, G. (2013). Global river hydrography and network routing: Baseline data and new approaches to study the world's large river systems. *Hydrological Processes*, *27*(15), 2171–2186. https://doi.org/10.1002/hyp.9740

Li, Y., Cheng, Y., Zhou, L., & Yang, Y. (2021). Advances, norms, and perspectives in product chemical footprint research. *International Journal of Environmental Research and Public Health*, *18*(5), 2728. https://doi.org/10.3390/2Fijerph18052728

Linke, S., Lehner, B., Ouellet Dallaire, C., Ariwi, J., Grill, G., Anand, M., Beames, P., Burchard-Levine, V., Maxwell, S., Moidu, H., Tan, F., & Thieme, M. (2019). Global hydro-environmental sub-basin and river reach characteristics at high spatial resolution. *Scientific Data*, *6*, 283. https://doi.org/10.1038/s41597-019-0300-6

Ma, X., Zuo, H., Tian, M., Zhang, L., Meng, J., Zhou, X., & Liu, Y. (2016). Assessment of heavy metals contamination in sediments from three adjacent regions of the Yellow River using metal chemical fractions and multivariate analysis techniques. *Chemosphere*, *144*, 264–272. https://doi.org/10.1016/j.chemosphere.2015.08.026

Makarova, A., Shlyakhov, P., & Tarasova, N. (2018). Estimating chemical footprint on high-resolution geospatial grid. *Procedia CIRP*, *69*(1), 469–474. https://doi.org/10.1016/j.procir.2018.01.001

Marzullo, R. D. C. M., dos Santos Matai, P. H. L., & Morita, D. M. (2018). New method to calculate water ecotoxicity footprint of products: A contribution to the decision-making process toward sustainability. *Journal of Cleaner Production*, *188*, 888–899. https://doi.org/10.1016/j.jclepro.2018.03.307

MDEQ. (2015). *Michigan TENORM Disposal Advisory Panel* [White Paper, 2014–2015]. Michigan Department of Environmental Quality. https://www.michigan.gov/documents/deq/deq-RMG-TENORM_Disposal_Advisory_Panel_White_Paper_-_FINAL_481404_7.pdf

Paulillo, A., Clift, R., Dodds, J. M., Milliken, A., Palethorpe, S. J., & Lettieri, P. (2020). Radiological impacts in Life Cycle Assessment. Part I: General framework and two practical methodologies. *Science of The Total Environment*, *708*, 135179. https://doi.org/10.1016/j.scitotenv.2019.135179

Pebesma, E. (2018). Simple features for R: Standardized support for spatial vector data. *The R Journal*, *10*(1), 439–446. https://doi.org/10.32614/RJ-2018-009

Perry, S. G., Cimorelli, A. J., Paine, R. J., Brode, R. W., Weil, J. C., Venkatram, A., Wilson, R. B., Lee, R. F., & Peters, W. D. (2005). AERMOD: A dispersion model for industrial source applications. Part II: Model performance against 17 field study databases. *Journal of Applied Meteorology*, *44*(5), 694–708.

Posthuma, L., Bjørn, A., Zijp, M. C., Birkved, M., Diamond, M. L., Hauschild, M. Z., & Van de Meent, D. (2014). Chemical footprints: Thin boundaries support environmental quality management. *Environmental Science & Technology*, *48*(22), 13025–13026. https://doi.org/10.1021/es505004n

Pre Consultants. (2018). Simapro Version 8.5.2.

R Core Team. (2017). R: A Language and Environment for Statistical Computing (Version 3.4.3 (2017-11-30). Vienna, Austria. https://www.R-project.org/

Rosenbaum, R. K., Bachmann, T. M., Gold, L. S., Huijbregts, M. A., Jolliet, O., Juraske, R., & Hauschild, M. Z. (2008). USEtox—the UNEP-SETAC toxicity model: Recommended characterisation factors for human toxicity and freshwater ecotoxicity in life cycle impact assessment. *The International Journal of Life Cycle Assessment*, *13*(7), 532–546. https://doi.org/10.1007/s11367-008-0038-4

Sala, S., & Goralcyk, M. (2013). Chemical footprint: A methodological framework for bridging life cycle assessment and planetary boundaries for chemical pollution. *Integrated Environmental Assessment and Management*, *9*(4), 623–632. https://doi.org/10.1002/ieam.1471

Saouter, E., Aschberger, K., Fantke, P., Hauschild, M. Z., Bopp, S. K., Kienzler, A., Paini, A., Pant, R., Secchi, M., & Sala, S. (2017). Improving substance information in USEtox®, part 1: Discussion on data and approaches for estimating freshwater ecotoxicity effect factors. *Environmental Toxicology and Chemistry*, *36*(12), 3450–3462. https://doi.org/10.1002/etc.3889

Sprecher, B., Xiao, Y., Walton, A., Speight, J., Harris, R., Kleijn, R., Visser, G., & Kramer, G. J. (2014). Life cycle inventory of the production of rare earths and the subsequent production of NdFeB rare earth permanent magnets. *Environmental Science & Technology*, *48*, 3951–3958. https://doi.org/10.1021/es404596q

Steffen, W., Richardson, K., Rockström, J., Cornell, S. E., Fetzer, I., Bennett, E. M., & Folke, C. (2015). Planetary boundaries: Guiding human development on a changing planet. *Science*, *347*(6223), 1259855. https://doi.org/10.1126/science.1259855

Treyer, K., & Bauer, C. (2016). Life cycle inventories of electricity generation and power supply in version 3 of the ecoinvent database—part II: Electricity markets. *International Journal of Life Cycle Assessment*, *21*, 1255–1268. https://doi.org/10.1007/s11367-013-0694-x

Vanham, D., Leip, A., Galli, A., Kastner, T., Bruckner, M., Uwizeye, A., & Hoekstra, A. Y. (2019). Environmental footprint family to address local to planetary sustainability and deliver on the SDGs. *Science of the Total Environment*, *693*, 133642. https://doi.org/10.1016/j.scitotenv.2019.133642

Verones, F., Hellweg, S., Antón, A., Azevedo, L. B., Chaudhary, A., Cosme, N., & Huijbregts, M. A. (2020). LC-IMPACT: A regionalized life cycle damage assessment method. *Journal of Industrial Ecology*, *24*(6), 1201–1219. https://doi.org/10.1111/jiec.13018

Wang, L. L. (2019). *Methodology for Accounting for the Chemical Footprint of Products Based on Regional Toxic Stress Indices, China*, (Zhejiang, CN CN201811009866.3). Hangzhou Huiliang Intellectual Property Agency Co., Ltd. 33259. http://d.wanfangdata.com.cn/patent/CN201811009866.3

Worldsteel. (2020). Chinese mainland steel plants 2020. Worldsteel Association. Available for purchase at https://www.worldsteel.org/publications/bookshop.html

Zijp, M. C., Posthuma, L., & van de Meent, D. (2014). Definition and applications of a versatile chemical pollution footprint methodology. *Environmental Science & Technology*, *48*(18), 10588–10597. https://doi.org/10.1021/es500629f

